THE JOURNAL OF PHYSICAL CHEMISTRY B

Article

pubs.acs.org/JPCB

Comparative Proton Transfer Efficiencies of Hydronium and Hydroxide in Aqueous Solution: Proton Transfer vs Brownian Motion

Nizam Uddin,[†] Jeongmin Kim,[‡] Bong June Sung,*[,‡] Tae Hoon Choi,*[,§] Cheol Ho Choi,*[,†] and Heon Kang*[,∥]

[†]Department of Chemistry and Green-Nano Materials Research Center, College of Natural Sciences, Kyungpook National University, Taegu 702-701, Republic of Korea

[‡]Department of Chemistry and Research Institute for Basic Science, Sogang University, Seoul 121-742, Republic of Korea

[§]Department of Chemical Engineering Education, Chungnam National University, Daejeon 305-764, Republic of Korea

[∥]Department of Chemistry, Seoul National University, 1 Gwanak-ro, Seoul 151-747, Republic of Korea

ABSTRACT: With the help of QM/EFP-MD with modern correlated quantum theories, distinctly different proton transport dynamics for hydronium and hydroxide ions was revealed. The efficiency of proton transfer for hydronium was found to be significantly higher than that for hydroxide, and the difference in efficiency increased as the temperature was lowered. This difference in dynamics suggests that molecular Brownian diffusion may play an important role in hydroxide transport. Our theoretical findings are consistent with recent experimental observations of proton transfer in amorphous solid water.

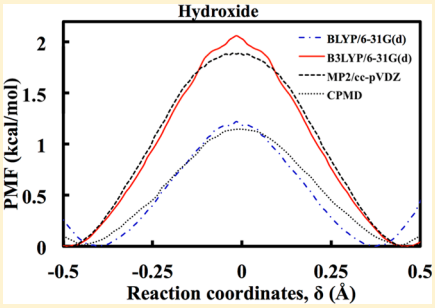

I. INTRODUCTION

Hydronium (H_3O^+) and hydroxide (OH^-) transport in aqueous solutions has been a subject of intense research in recent years due to its fundamental significance in many chemical and biochemical processes ranging from simple acid−base reactions to enzymatic functions.[1−23] It is well-known that the diffusion coefficients of hydronium and hydroxide ions are anomalously large and that the mobility of a hydronium ion is nearly twice that of a hydroxide ion at room temperature, which led to Grotthuss' concept of proton transfer via structural diffusion.

Extensive theoretical studies using Car−Parrinello molecular dynamics (CPMD),[14,24−27] extended valence bond (EVB) theory,[28−30] reactive molecular dynamics,[31] and the dissociating model[32] have been performed to illuminate the intriguing transport features of these ions. Accordingly, it has been well established that the proton transfer mechanism of hydronium involves an intricate interplay between the Eigen cation, $H_3O^+(H_2O)_3$, and Zundel cation, $[H_2O\cdots H\cdots OH_2]^+$.[1−7] It has been presumed that hydroxides also undergo such proton transfer,[8−12] although their critical solvation structures and related proton transfer mechanisms are quite controversial.[1−7,13−16] A recent comprehensive review by Marx et al.[13] proposed three possible hydroxide diffusion mechanisms via proton transfer: mirror image, dynamical hypercoordination, and static hypercoordination mechanisms. However, the mechanism determined from theoretical investigations strongly depends on the choice of exchange-correlation functionals used in the CPMD simulations.

Following the terminology of Hynes, Borgis, and others,[33−36] proton transfer in aqueous solutions is in general associated with a separating reaction barrier within the Born−Oppenheimer approximation. Depending on barrier heights,[34−39] proton transfer can be classified as either adiabatic or nonadiabatic due to the quantum tunnel splitting effect. In the limit of adiabatic proton transfer,[33,40] the energy separation of ground and excited proton transfer vibrational states is large enough to prevent a significant population of excited states, as is the case when the potential energy barrier is small or nonexistent. On the other hand, nonadiabatic proton transfer becomes especially important at low temperatures, where the proton transfer barrier is much higher than the thermal energy. Therefore, obtaining an accurate potential energy or free energy barrier of proton transfer in solution is critical. Contrasting to its importance, traditional high level *ab initio* correlation theories have not been well adopted for the study of hydronium and hydroxide dynamics in solution.

Diffusion coefficients represent collectively the dynamics of various transport events such as proton hopping, molecular diffusion, thermal rattling, hydrogen bonding, rotational relaxations, and solvation shell dynamics. To model various transport events with energetically reliable accuracies, long-time quantum mechanical molecular dynamics simulations with high level correlation theories are desirable. Recently, a hybrid quantum mechanical/effective fragment potential (QM/EFP)

Received: September 15, 2014
Revised: October 31, 2014
Published: November 3, 2014

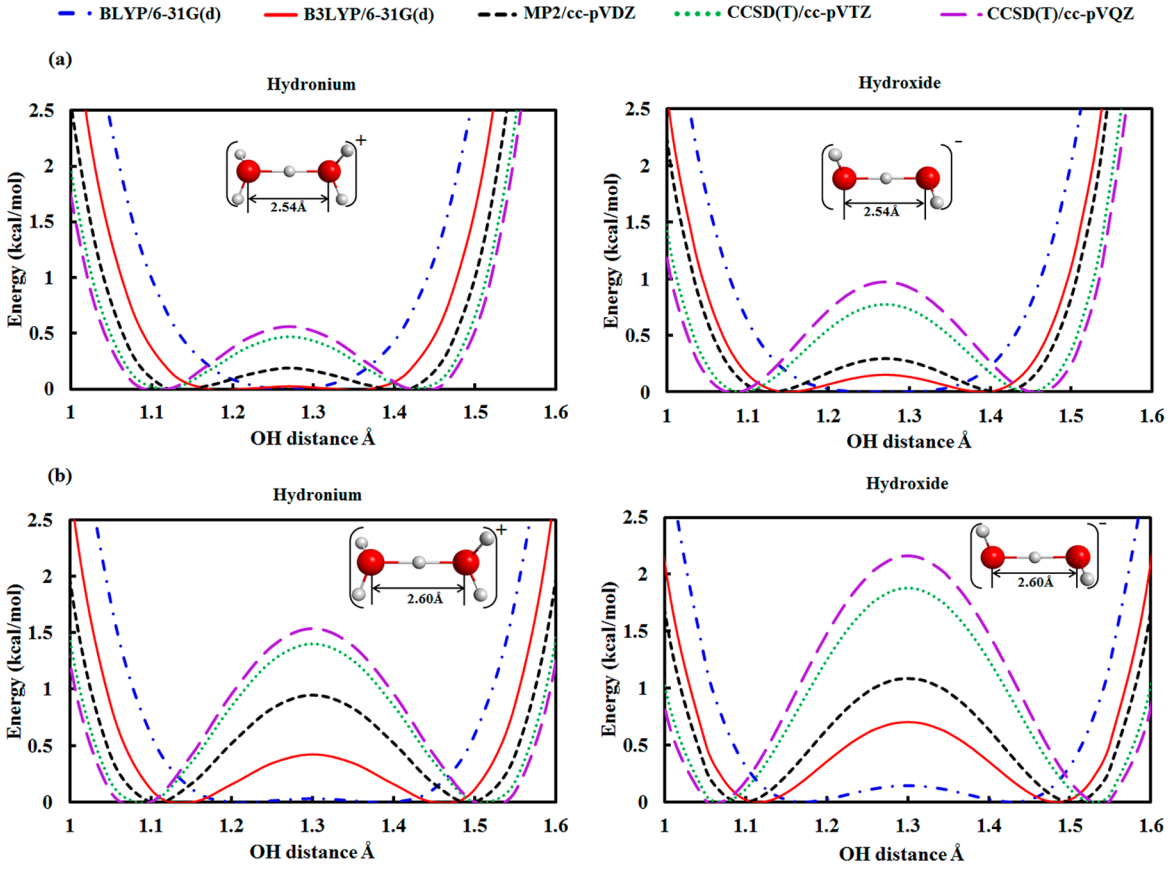

Figure 1. Potential energy surfaces of $H_5O_2^+$ and $H_3O_2^-$ as a function of the shared proton for a fixed O−O distance of (a) 2.54 and (b) 2.60 Å. Results were obtained at the BLYP/6-31G(d), B3LYP/6-31G(d), MP2/cc-pVDZ, CCSD(T)/cc-pVTZ, and CCSD(T)/cc-pVQZ levels of theory.

scheme within the Born−Oppenheimer approximation has been suggested for practical quantum mechanical MD simulations.[41] The EFP[42] is a fully *ab initio* force field composed of sophisticated Coulomb, polarization, exchange repulsion, dispersion, and charge transfer terms. Detailed descriptions of the EFP and pertinent references can be found in a recent paper by Gordon et al.[43] The hybrid QM/EFP-MD method has been successfully utilized in various solution dynamics studies, including proton transfer.[44−47]

Experimental studies of the microscopic dynamics of hydroxide ion diffusion in an aqueous solution have been relatively scarce[15,20] due to the difficultly in identifying the transitory structures of hydroxide ion diffusion through spectroscopic methods. Using femtosecond spectroscopy, Thøgersen et al.[15] showed that the reorientation time of OH^- ions in water has a drastic temperature dependence, especially at low temperatures, implying that structural diffusion events are significantly suppressed. Later, Ma and Tuckerman[48] suggested an explanation for this observation using CPMD simulations by showing that proton transfer events were suppressed by a pronounced population change of the dominant aqueous OH^- solvation complexes at low temperatures. Recently, the diffusion of hydronium and hydroxide ions has been studied experimentally in amorphous solid water (ASW) at low temperatures,[49] which showed that the ions move via intrinsically different mechanisms in ASW. Although hydronium ions hop via an efficient proton transfer, hydroxide ions move via Brownian molecular diffusion. This new experimental finding strongly suggests the importance of the molecular diffusion mechanism, especially in the case of hydroxide transport, which has been neglected thus far. Since ASW and liquid water have certain similarities in molecular packing structures and thermodynamic properties,[50] an intriguing question is to what extent the different transport mechanisms are transferable to hydronium and hydroxide ions in aqueous solution at room temperature. Hence, the present report explores the comparative proton transfer efficiencies of hydronium and hydroxide ions in aqueous solution using both *ab initio* quantum calculations on molecular clusters and QM/EFP-MD simulations. The consequent competition between proton transfer and molecular Brownian motion in the two ion transport systems is also discussed.

II. COMPUTATIONAL DETAILS

Density functional theory using BLYP and the exact exchange-incorporated B3LYP functional was adopted using 6-31G(d) basis sets to estimate proton transfer barriers for $H_5O_2^+$ and $H_3O_2^-$ model clusters. In addition, traditional correlated theories such as MP2[51] and CCSD(T)[52] were also adopted using cc-pVDZ, cc-pVTZ, and cc-pVQZ correlation consistent basis sets. Quantum mechanical/molecular dynamics simulations were also performed for hydronium and hydroxide diffusion by employing our quantum mechanical/effective fragment potential molecular dynamics (QM/EFP-MD) method.[41] The advantages of QM/EFP-MD are as follows: (i) the hybrid QM-EFP method can significantly reduce computational overhead, (ii) the *ab initio* driven EFP offers a high computational accuracy, and (iii) the calculation of the QM region can be improved by utilizing various advanced quantum chemical theories in combination with traditional

dx.doi.org/10.1021/jp5093114 | J. Phys. Chem. B 2014, 118, 13671−13678

atom-center Gaussian basis sets. In the present work, canonical QM/EFP-MD simulations were performed for excess hydronium and hydroxide ions in a condensed water model. Spherical QM/EFP models of $O_6H_{13}^+$ and $O_7H_{13}^-$ QM regions were prepared with 286 and 285 explicit EFP water molecules, respectively. MD simulations were performed at 160 and 300 K, where the former condition possibly represents supercooled water or ASW. In order to prevent the evaporation of water during long-time simulations, a harmonic restraint potential for the solvent boundary was applied. Spherical boundary models with ∼300 EFP waters have been verified as a good model for condensed phase simulation in our previous papers,[44] in which we have shown that the results of our spherical boundary models are nearly identical to those of periodic boundary models. The size of the QM region was designed by explicitly adding water molecules one at a time near the charged ion (hydronium or hydroxide) until the radial distribution functions (RDFs or $g(r)$) and potential of mean force (PMF) converged. Since we were using fixed QM boundary for the QM/EFP, it is possible that the chances of proton transfer to EFP are discouraged. However, the convergence of the radial distribution functions as well as potential of mean forces as a function of QM water ensures that the proton transfer occurs within QM region during our simulation time. We employed the BLYP/6-31G(d), B3LYP/6-31G(d), and MP2/cc-pVDZ levels of theory for the QM region during the MD simulations. Since the comparisons against earlier CPMD studies are important parts of current studies, we adopt the same BLYP functional. In addition, B3LYP was also chosen for its exact exchange functional. Canonical NVT simulations were performed for more than 100 ps in addition to the initial NVE equilibrations with 1 fs time steps. A Nosé−Hoover thermostat was employed during the NVT simulations. All calculations were performed with a modified version of GAMESS.[53]

III. RESULTS AND DISCUSSION

A. Quantum Mechanical Calculations on Small Ion Clusters. The proton transfer barriers of $H_5O_2^+$ and $H_3O_2^-$ were investigated by calculating the single point energy as a function of the location of the proton transferring between the two O atoms. In the proton transfer mechanism, the H^+ of H_3O^+ is transferred to H_2O while the H^+ of H_2O is transferred to OH^-. The geometries of $H_5O_2^+$ and $H_3O_2^-$ at each location were first optimized at the MP2/cc-pVDZ level of theory. In order to introduce solvation effects to the transferring proton, the calculations were performed at O−O distances of 2.54 and 2.60 Å. The shared proton was displaced along the line joining the two O atoms while keeping all other degrees of freedom fixed. Figure 1 shows the potential energy curves of proton transfer as calculated with BLYP, B3LYP, MP2, and CCSD(T), where the curves of CCSD(T) serve as references. Basis set convergence is seen from the values of CCSD(T) with the cc-pVTZ and cc-pVQZ basis sets. The proton transfer barriers of $H_5O_2^+$ are consistently lower than those of $H_3O_2^-$ for all theories. Among the results, the BLYP functional, which does not include exact exchange, yielded negligible barriers, irrespective of ion type and O−O distance. These results are especially distinct when the BLYP values are compared against the CCSD(T) results. The underestimation of reaction barriers by density functional theory without exact exchange has been well documented in the literature.[54−57] In contrast, the B3LYP values are closer to those of MP2, indicating that the inclusion of exact exchange improves the accuracy in calculations of reaction barriers. The predicted barrier heights of hydronium and hydroxide are comparable to the average thermal energy of 0.59 kcal/mol at 300 K, indicating relatively small tunneling effects.

As compared with potential energy surfaces found by static quantum mechanical calculations, free energy surfaces obtained from molecular dynamics simulations involve various dynamical effects. Therefore, it is not straightforward to assume that the same dependency on computational theory can be applied to the free energy barriers of proton transfer. Therefore, QM/EFP-MD simulations were also performed on hydronium and hydroxide transport dynamics, and the results are discussed in the following section.

B. QM/EFP-MD Simulations on Hydronium and Hydroxide Transport in Solution. We performed canonical QM/EFP-MD simulations for excess hydronium and hydroxide ions in water at 160 and 300 K as described in the Computational Details section using three different quantum theories for the QM region: BLYP/6-31G(d), B3LYP/6-31G(d), and MP2/cc-pVDZ. The resulting PMFs for hydronium and hydroxide along the proton transfer paths at 300 K are shown in Figure 2. The proton transfer coordinate is represented by δ, $|\delta| = \min|r_{O^*-H} - r_{O_w-H}|$, where O* is the oxygen atom of either hydronium or hydroxide and O_w represents the oxygen atom of water. When we compare our QM/EFP-MD simulations based on BLYP/6-31G(d) with previous BLYP-based CPMD simulations,[58,14] we found that the two methods produce similar PMFs for hydronium and hydroxide transfer. This shows that the QM/EFP-MD and CPMD simulations are consistent when the same exchange-correlation functionals are used, even though the two methods have significantly different computational procedures. On the other hand, the QM/EFP-MD simulations using both B3LYP/

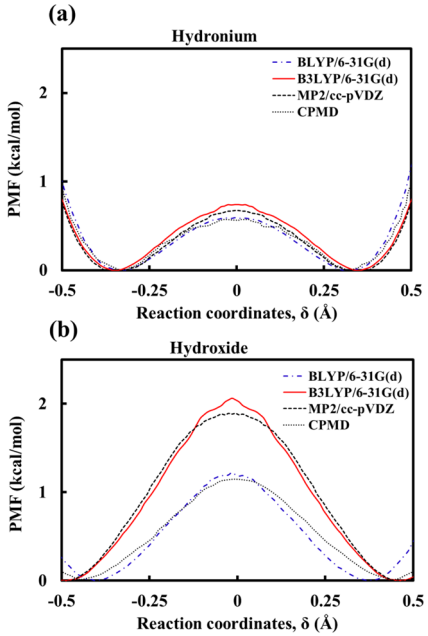

Figure 2. Potential of mean forces (PMF) for hydronium and hydroxide systems generated from QM/EFP-MD simulations using BLYP/6-31G(d), B3LYP/6-31G(d), and MP2/cc-pVDZ levels of theory for the QM region. CPMD simulation data are taken from refs 14 and 58.

dx.doi.org/10.1021/jp5093114 | J. Phys. Chem. B 2014, 118, 13671−13678

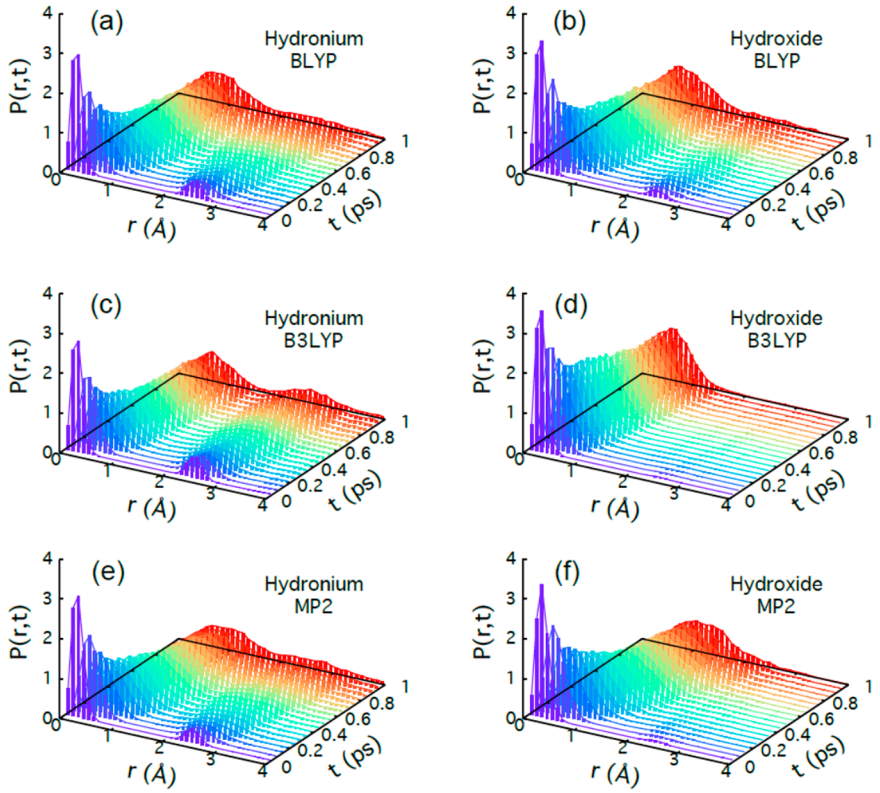

Figure 3. $P(r,t)$s of the oxygen atoms of hydronium and hydroxide as a function of r for various times t obtained from the QM/EFP-MD simulations using BLYP, B3LYP, and MP2 for the QM region.

6-31G(d) and MP2/cc-pVDZ predicted consistently higher free energy barriers than BLYP/6-31G(d) and CPMD. The difference is especially large in the case of hydroxide (0.7−0.9 kcal/mol). The discrepancy between these two groups of calculations (B3LYP and MP2 versus BLYP) was also seen in the potential energy barriers in the previous section (Figure 1). Therefore, the potential energy barriers of proton transfer have a determining effect on the free energy barriers. Consequently, it is reasonable to expect that CCSD(T) could yield even higher free energy barriers. Therefore, our results contradict the previous fluxional idea of negligible barrier,[14] especially in the case of hydroxide.

Clearly different free energy barriers for hydronium and hydroxide were observed from the QM/EFP-MD simulations only with B3LYP and MP2. According to these results, hydronium diffusion has a lower free energy barrier (by ∼1.3 kcal/mol) and a narrower barrier width (by 0.2 Å) than hydroxide, which makes proton transfer with hydronium much easier. After adding nuclear quantum effect corrections to the CPMD simulations, the barriers for proton transfer with hydronium and hydroxide reduced to 0.1 and 0.3 kcal/mol, respectively,[13] making the difference between the free energy barriers of the two ions negligible. Similar nuclear quantum effect corrections would certainly reduce the free energy barriers of our B3LYP and MP2 computations. However, the effects would not be significant, since the barrier heights are near the average thermal energy at 300 K. It should also be noted that the potential energy barriers of proton transfer were even higher with the more accurate CCSD(T) theory, implying free energy barriers as obtained with CCSD(T) would be higher than those found with B3LYP and MP2. The effect of the difference in the free energy barrier heights on the transport dynamics is discussed in the next section.

C. Space-Time Correlation Functions for Multiple Transport Paths. While previous theoretical studies focused on structural and thermodynamic aspects of proton transfer mechanisms, they often do not include dynamic information. We calculated the van Hove space-time correlation functions, $G_s(r,t) \equiv \langle \delta[\mathbf{r} - \mathbf{r}_O(t) + \mathbf{r}_O(0)] \rangle$, of the oxygen atoms in hydronium and hydroxide to determine the space-time correlation of the target oxygen. Here, $\mathbf{r}_O(t)$ denotes the position vector of the target oxygen, where r is the size of vector $\mathbf{r}$. The term $4\pi r^2 G_s(r,t) \equiv P(r,t)$ is the probability that an oxygen atom is at position r at time t given that the oxygen atom was at the origin at $t = 0$. Note that unlike the conventional estimation of the $G_s(r,t)$ of single molecules, we keep track of the ion charges and calculate $G_s(r,t)$ from the position vectors of charged molecules. For example, when a proton transfers from molecule 1 to molecule 2, we record the position vector of molecule 2 instead of molecule 1. For Brownian particles, $G_s(r,t)$ takes a simple Gaussian function. Otherwise, $G_s(r,t)$ shows non-Gaussian behavior often with additional peaks, indicating the presence of spatially heterogeneous dynamics or multiple transport mechanisms. Figure 3 shows the $P(r,t)$s of the oxygen atoms in hydronium and hydroxide at 300 K obtained from QM/EFP-MD simulations with BLYP, B3LYP, and MP2 for the QM region. For hydronium, regardless of the quantum theory used, the $P(r,t)$s clearly show two peaks (Figures 3a,c,e). Such doubly peaked $P(r,t)$s when $t < 0.2$ ps indicate that there are two distinct transport mechanisms for hydronium ions. The first peak around 0.2 Å accounts for the thermal rattling of hydronium ions, while the second peak around 2.4 Å represents

dx.doi.org/10.1021/jp5093114 | J. Phys. Chem. B 2014, 118, 13671−13678

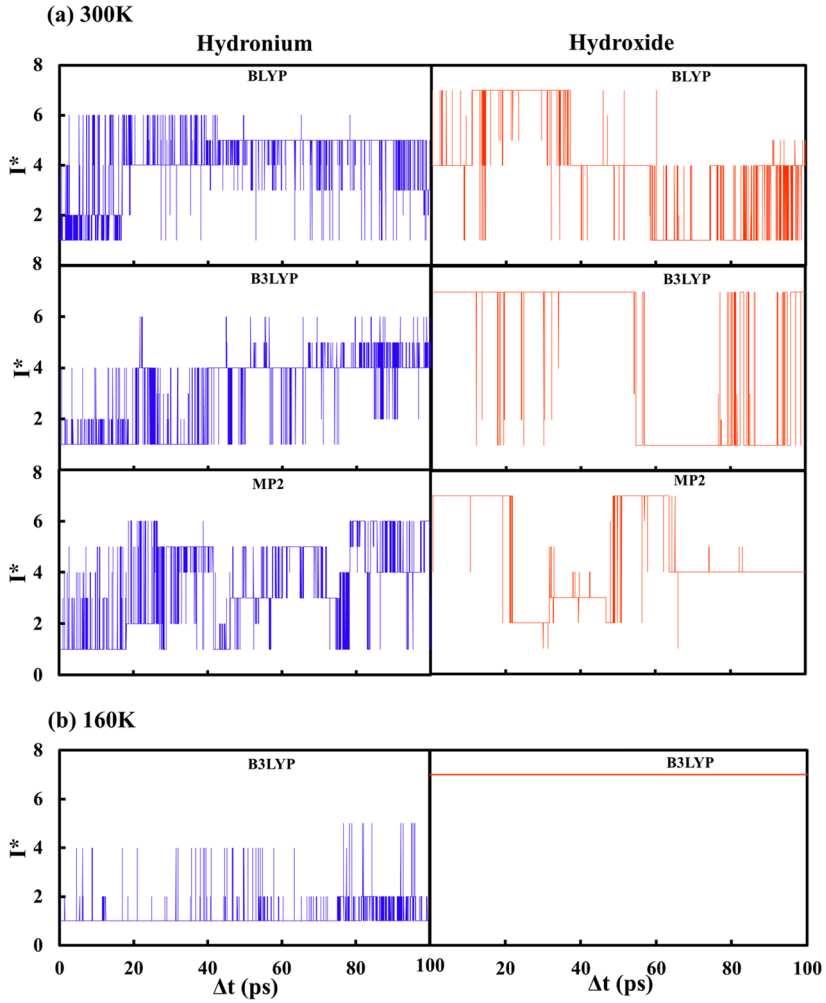

Figure 4. Time dependence of the indices (I*) of the H_3O^+ and OH^- oxygen O*. The 100 ps trajectories were calculated with (a) BLYP, B3LYP, and MP2 at 300 K and (b) B3LYP at 160 K.

proton transfer. The large intensity of the second peak when $t <$ 0.2 ps indicates the occurrence of fast proton transfer, whose time scale is consistent with recent experimental results.[19] After t = 0.5 ps, hydronium may diffuse longer distances via thermal motion, causing an overlap of the two peaks. In the case of hydroxide, the $P(r,t)$s show different behaviors depending on the quantum theory employed in the QM/EFP-MD simulations. When BLYP is employed (Figure 3b), the second $P(r,t)$ peak is still observed even though its height is smaller than that of hydronium. This suggests that proton transfer still occurs readily for hydroxide, though the process is not as efficient as it is for hydronium. More interesting is that the second $P(r,t)$ peak is hardly observed when B3LYP and MP2 are employed. This alternatively suggests that proton transfer would hardly occur within a time scale of 1 ps even at 300 K, which is very different from the current view of efficient proton transfer mechanism in hydroxide diffusion. Consequently, it is clear that 1 kcal/mol barrier height difference between hydronium and hydroxide in free energy scale dramatically changes the dynamics of proton transfer. Although we adopted relatively low levels of theory (B3LYP and MP2) for QM region, the fact that they exhibited consistent results justifies their validity.

D. Dynamic Properties of the Temperature Dependency of Proton Transfer. To gain insight into the proton transfer mechanism, the identities of the hydronium and hydroxide oxygen were tracked during the MD simulations. Figure 4 shows the time profiles of the indices (I*), the identities of the H_3O^+ or OH^- oxygen (O*). At room temperature (300 K), the thick lines are more pronounced in hydronium, indicating that proton transfer is carried out more frequently in hydronium than in hydroxide. Proton hopping in hydroxide, determined by BLYP, is relatively more frequent than that determined by B3LYP or MP2, which is a consequence of the lower barrier heights found with BLYP, as seen in Figures 1 and 2. We also performed QM/EFP-MD simulations at a low temperature (160 K) at the B3LYP/6-31G(d) level of theory to simulate amorphous solid water (Figure 4b). Proton transfer in hydronium still occurs on a fast time scale, although the hopping frequency slightly decreased at the low temperature. On the other hand, proton transfer in hydroxide at 160 K never occurred within the 100 ps time scale.

For further statistical investigation into the proton transfer dynamics, survival probabilities $\langle C(t)\rangle$ (the fraction of ions that do not undergo proton transfer until time t) at 160 and 300 K were also estimated and are shown in Figure 5. For each ion, the survival probability was initially $C(t{=}0) = 1$. $C(t)$ becomes zero when proton transfer occurs; otherwise, $C(t)$ remains 1. Figure 5a depicts the $\langle C(t)\rangle$s obtained from the QM/EFP-MD simulations with B3LYP/6-31G(d) at 160 and 300 K. At 160 K,

dx.doi.org/10.1021/jp5093114 | J. Phys. Chem. B 2014, 118, 13671−13678

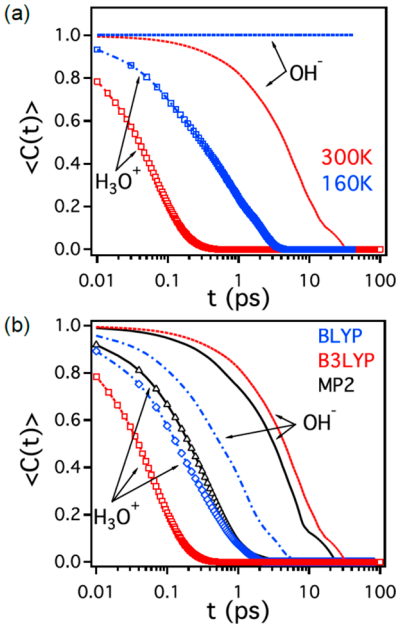

Figure 5. (a) Survival probability $\langle C(t)\rangle$ of hydronium and hydroxide as a function of time at 300 and 160 K obtained from QM/EFP-MD simulations using B3LYP/6-31G(d) for the QM region. (b) $\langle C(t)\rangle$ of hydronium and hydroxide at 300 K obtained using BLYP/6-31G(d) (blue), B3LYP/6-31G(d) (red), and MP2/cc-pVDZ (black). $\langle C(t)\rangle$ denotes the fraction of protons that stay with the original molecules without hopping until time *t*.

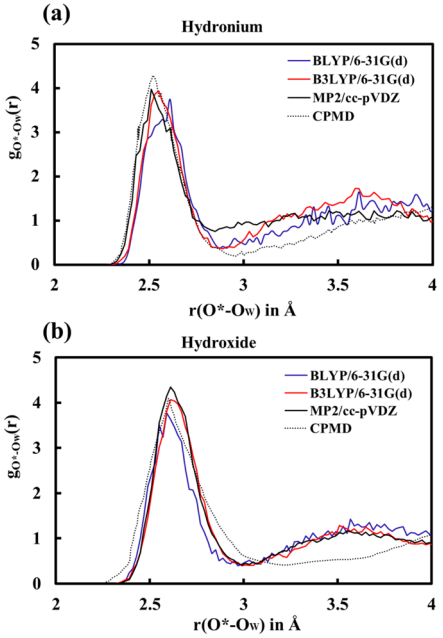

Figure 6. Radial distribution functions (RDFs) of (a) hydronium and (b) hydroxide obtained from the QM/EFP-MD simulations using BLYP, B3LYP, and MP2 for the QM region. CPMD simulation data are taken from refs 14 and 58.

$\langle C(t)\rangle$ does not decay for hydroxide, indicating that hydroxide hardly undergoes proton transfer within 100 ps. Conversely, proton transfer occurs for about 80% of the hydronium ions at t = 1 ps, i.e., $\langle C(t = 1\ \text{ps})\rangle \cong 0.2$. This result is in good agreement with the experimental studies of ASW, which did not show proton transfer during hydroxide diffusion through an ASW film at 155−175 K, in contrast to the efficient proton transfer of hydronium.[49] As the temperature increases to 300 K, both hydronium and hydroxide are more likely to undergo proton transfer. However, proton transfer for hydronium is much more efficient than that for hydroxide. For example, when t = 0.1 ps, about 80% of the hydronium ions experience proton transfer whereas only a small fraction of the hydroxide ions undergo proton transfer.

Figure 5b compares the $\langle C(t)\rangle$s obtained using different levels of quantum theories. Regardless of the quantum theory used, $\langle C(t)\rangle$ decays faster for hydronium than for hydroxide, indicating that proton transfer occurs more readily for hydronium ions. According to simulations using B3LYP and MP2, the $\langle C(t)\rangle$ of hydroxide decays more slowly *by orders of magnitude* than that of hydronium, which is consistent with the simulation results for $P(r,t)$. On the other hand, the $\langle C(t)\rangle$ of hydroxide obtained using BLYP in the QM/EFP-MD simulations decays relatively quickly, implying spuriously fast proton transfer.

E. Statistical Analysis of Solvation Structures. It is helpful to investigate the solvation structure around proton transfer events. Figure 6 shows the radial distribution functions (RDFs), $g_{O^*-Ow}(r)$, for hydronium and hydroxide generated with QM/EFP-MD simulations using three different quantum theories: BLYP, B3LYP, and MP2. The first peaks in the solvation of hydronium calculated with the three different QM theories are nearly identical and agree well with that found by CPMD.[58] In the solvation of hydroxide, the first peaks calculated with QM/EFP-MD using the BLYP functional and previous CPMD simulations were slightly shifted to the left (O_w is held closer to O*) compared with those calculated at the B3LYP and MP2 levels of theory. This is in agreement with observations from the PMF analysis shown in Figure 2b. Although the first peak found by CPMD for hydroxide[14] is slightly broader than those found by QM/EFP-MD, the overall shapes and heights are similar, which indicates a close correspondence between our QM/EFP-MD results and the CPMD simulations for at least the first solvation structure.

To investigate the solvation pattern in detail, the coordination number (CN) of the proton-receiving oxygen (O_w) was analyzed. Figure 7 shows the probability distribution of the CNs in the first solvation shell, which indicates the number of hydrogen bonds accepted by O*. Hydronium ions mostly accept three hydrogen bonds in all QM/EFP-MD simulations. However, the most probable CN for hydroxide in simulations with B3LYP and MP2 is four, whereas simulations with BLYP still favor 3-fold coordination. When proton transfer occurs ($|\delta| \leq 0.1$ Å, corresponding to a nearly symmetric Zundel-like structure), as shown in Figure 7c, the most probable CN changes from four to three. Thus, the hydroxide ion becomes less solvated near a proton transfer event. The reduced CN during proton transfer is consistent with the dynamical hypercoordination suggested by previous CPMD simulations.[13]

IV. CONCLUSION

The quantum mechanical theories of BLYP, B3LYP, MP2, and CCSD(T) were adopted to estimate the proton transfer barriers of $H_5O_2^+$ and $H_3O_2^-$ model clusters. Compared with CCSD(T)/cc-pVQZ, BLYP/6-31G(d), which does not include exact exchange functional, significantly underestimates the proton transfer barriers. On the other hand, the results of B3LYP are consistent with those of MP2, indicating the

dx.doi.org/10.1021/jp5093114 | J. Phys. Chem. B 2014, 118, 13671−13678

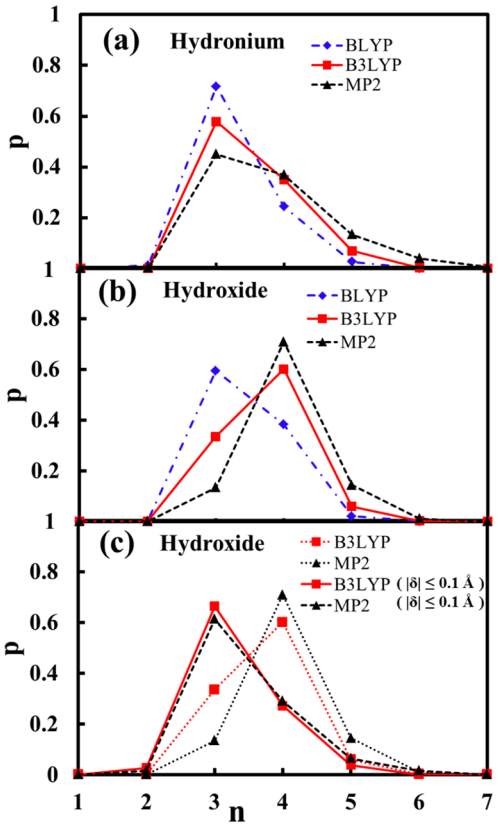

Figure 7. Probability distribution of the number of hydrogen bonds accepted by the oxygen atoms, O*, of (a) hydronium and (b) hydroxide. (c) Hydroxide simulations with B3LYP and MP2 when the probability distributions are close to the proton transfer events ($|\delta| \leq 0.1$ Å).

importance of including exact exchange functional. Similar to the model cluster calculations, the transport dynamics depended on the computational theory. Specifically, MD simulation with the BLYP functional largely underestimated the proton transfer free energy barrier of hydroxide as compared with the other theories, which resulted in a spuriously efficient proton transfer for hydroxide. In contrast, the MD simulations with B3LYP and MP2 clearly showed the importance of Brownian motion in hydroxide transport.

In brief, contrasting to the previous assumptions, the present comparative study shows that the proton transfer efficiency of hydroxide is significantly lower than that of hydronium. Consequently, at room temperature, Brownian molecular diffusion may have an important contribution to the transport and reaction of hydroxide ions. Furthermore, at a low temperature (160 K), hydroxide migrates exclusively via Brownian motion without proton transfer, which is consistent with recent experimental studies of hydroxide diffusion in ASW at 155−175 K.[49] This is in stark contrast to the proton-transfer-dominated hydronium transport, which shows rapid proton oscillation on the picosecond time scale at both 300 and 160 K. The present findings imply that acids and bases may have quite different acting mechanisms and ranges in aqueous solutions due to their different diffusion mechanisms.

AUTHOR INFORMATION

Corresponding Authors

*E-mail bjsung@sogang.ac.kr (B.J.S.).
*E-mail thchoi@cnu.ac.kr (T.H.C.).
*E-mail cchoi@knu.ac.kr (C.H.C.).
*E-mail surfion@snu.ac.kr (H.K.).

Author Contributions

N.U. and J.K. contributed equally to this work.

Notes

The authors declare no competing financial interest.

ACKNOWLEDGMENTS

This work was supported by a National Research Foundation grant funded by the Korean government (MSIP) (Project Nos. 2007-0056095, 2012-0004812, and 2013R1A1A2008403) and by the Samsung Science and Technology Foundation (SSTF-BA1301-04, HK).

REFERENCES

(1) Eigen, M.; de Maeyer, L. Self-Dissociation and Protonic Charge Transport in Water and Ice. *Proc. R. Soc. A* **1958**, *247*, 505−533.
(2) Eigen, M. Proton Transfer, Acid-Base Catalysis, and Enzymatic Hydrolysis. Part I: Elementary Processes. *Angew. Chem., Int. Ed. Engl.* **1964**, *3*, 1−19.
(3) Zundel, G.; Metzger, H. Die Hydratation Der Polystyrol-Sulfonsäure, Eine IR-Spektroskopische Untersuchung. *Z. Phys. Chem.* **1968**, *59*, 225−241.
(4) Marx, D. Proton Transfer 200 Years After Von Grotthuss: Insights From Ab Initio Simulations. *ChemPhysChem* **2006**, *7*, 1848−1870.
(5) Voth, G. A. Computer Simulation of Proton Solvation and Transport in Aqueous and Biomolecular Systems. *Acc. Chem. Res.* **2006**, *39*, 143−150.
(6) Chandra, A.; Tuckerman, M. E.; Marx, D. Connecting Solvation Shell Structure to Proton Transport Kinetics in Hydrogen−Bonded Networks via Population Correlation Functions. *Phys. Rev. Lett.* **2007**, *99*, 145901.
(7) Markovitch, O.; Chen, H.; Izvekov, S.; Paesani, F.; Voth, G. A.; Agmon, N. Special Pair Dance and Partner Selection: Elementary Steps in Proton Transport in Liquid Water. *J. Phys. Chem. B* **2008**, *112*, 9456−9466.
(8) Hückel, E. 3. Einzelvorträge: Elektrochemie. Theorie Der Beweglichkeiten Des Wasserstoff- Und Hydroxylions in Wässriger Lösung. *Z. Elektrochem.* **1928**, *34*, 546.
(9) Zatsepina, G. N. State of the Hydroxide Ion in Water and Aqueous Solutions. *J. Struct. Chem.* **1972**, *12*, 894−898.
(10) Schiöberg, D.; Zundel, G. Very Polarisable Hydrogen Bonds in Solutions of Bases Having Infra-Red Absorption Continua. *J. Chem. Soc., Faraday Trans. 2* **1973**, *69*, 771.
(11) Khoshtariya, D. E.; Berdzenishvili, N. O. A New Dynamic Elementary Act Model for Thermal and Photoinduced Proton Self-Exchange Through the Lyate Ion Hydrogen Bridges in Solutions. *Chem. Phys. Lett.* **1992**, *196*, 607−613.
(12) Agmon, N. Mechanism of Hydroxide Mobility. *Chem. Phys. Lett.* **2000**, *319*, 247−252.
(13) Marx, D.; Chandra, A.; Tuckerman, M. E. Aqueous Basic Solutions: Hydroxide Solvation, Structural Diffusion, and Comparison to the Hydrated Proton. *Chem. Rev.* **2010**, *110*, 2174−2216.
(14) Tuckerman, M. E.; Marx, D.; Parrinello, M. The Nature and Transport Mechanism of Hydrated Hydroxide Ions in Aqueous Solution. *Nature* **2002**, *417*, 923−925.
(15) Thøgersen, J.; Petersen, C. Reorientation of Hydroxide Ions in Water. *Chem. Phys. Lett.* **2008**, *466*, 1−5.
(16) Asthagiri, D.; Pratt, L. R.; Kress, J. D.; Gomez, M. A. Hydration and Mobility of HO-(Aq). *Proc. Natl. Acad. Sci. U. S. A.* **2004**, *101*, 7229−7233.
(17) Wooldridge, P. J.; Devlin, J. P. Proton Trapping and Defect Energetics in Ice From FT-IR Monitoring of Photoinduced Isotopic Exchange of Isolated D_2O. *J. Chem. Phys.* **1988**, *88*, 3086.

(18) Mohammed, O. F.; Pines, D.; Nibbering, E. T. J.; Pines, E. Base-Induced Solvent Switches in Acid−Base Reactions. *Angew. Chem., Int. Ed.* **2007**, *46*, 1458−1461.
(19) Woutersen, S.; Bakker, H. J. Ultrafast Vibrational and Structural Dynamics of the Proton in Liquid Water. *Phys. Rev. Lett.* **2006**, *96*, 138305.
(20) Roberts, S. T.; Ramasesha, K.; Petersen, P. B.; Mandal, A.; Tokmakoff, A. Proton Transfer in Concentrated Aqueous Hydroxide Visualized Using Ultrafast Infrared Spectroscopy. *J. Phys. Chem. A* **2011**, *115*, 3957−3972.
(21) Uritski, A.; Presiado, I.; Erez, Y.; Gepshtein, R.; Huppert, D. Temperature Dependence of Proton Diffusion in Ih Ice. *J. Phys. Chem. C* **2009**, *113*, 10285−10296.
(22) Cwiklik, L.; Devlin, J. P.; Buch, V. Hydroxide Impurity in Ice. *J. Phys. Chem. A* **2009**, *113*, 7482−7490.
(23) Mohammed, O. F.; Pines, D.; Dreyer, J.; Pines, E.; Nibbering, E. T. J. Sequential Proton Transfer Through Water Bridges in Acid-Base Reactions. *Science* **2005**, *310*, 83−86.
(24) Tuckerman, M.; Laasonen, K.; Sprik, M.; Parrinello, M. Ab Initio Molecular Dynamics Simulation of the Solvation and Transport of H_3O^+ and OH^- Ions in Water. *J. Phys. Chem.* **1995**, *99*, 5749−5752.
(25) Marx, D.; Tuckerman, M. E.; Hutter, J.; Parrinello, M. The Nature of the Hydrated Excess Proton in Water. *Nature* **1999**, *397*, 601−604.
(26) Asthagiri, D.; Pratt, L. R.; Kress, J. D. Ab Initio Molecular Dynamics and Quasichemical Study of H^+(aq). *Proc. Natl. Acad. Sci. U. S. A.* **2005**, *102*, 6704−6708.
(27) Bucher, D.; Gray-Weale, A.; Kuyucak, S. Ab Initio Study of Water Polarization in the Hydration Shell of Aqueous Hydroxide: Comparison Between Polarizable and Nonpolarizable Water Models. *J. Chem. Theory Comput.* **2010**, *6*, 2888−2895.
(28) Schmitt, U. W.; Voth, G. A. Multistate Empirical Valence Bond Model for Proton Transport in Water. *J. Phys. Chem. B* **1998**, *102*, 5547−5551.
(29) Schmitt, U. W.; Voth, G. A. The Computer Simulation of Proton Transport in Water. *J. Chem. Phys.* **1999**, *111*, 9361.
(30) Ufimtsev, I. S.; Kalinichev, A. G.; Martinez, T. J.; Kirkpatrick, R. J. A Multistate Empirical Valence Bond Model for Solvation and Transport Simulations of OH^- in Aqueous Solutions. *Phys. Chem. Chem. Phys.* **2009**, *11*, 9420−9430.
(31) Selvan, M. E.; Keffer, D. J.; Cui, S.; Paddison, S. J. A Reactive Molecular Dynamics Algorithm for Proton Transport in Aqueous Systems. *J. Phys. Chem. C* **2010**, *114*, 11965−11976.
(32) Lee, S. H.; Rasaiah, J. C. Proton Transfer and the Mobilities of the H^+ and OH− Ions From Studies of a Dissociating Model for Water. *J. Chem. Phys.* **2011**, *135*, 124505.
(33) Borgis, D.; Tarjus, G.; Azzouz, H. An Adiabatic Dynamical Simulation Study of the Zundel Polarization of Strongly H-Bonded Complexes in Solution. *J. Chem. Phys.* **1992**, *97*, 1390−1400.
(34) Borgis, D. C.; Lee, S.; Hynes, J. T. A Dynamical Theory of Nonadiabatic Proton and Hydrogen Atom Transfer Reaction Rates in Solution. *Chem. Phys. Lett.* **1989**, *162*, 19−26.
(35) Borgis, D.; Tarjus, G.; Azzouz, H. Solvent-Induced Proton Transfer in Strongly Hydrogen-Bonded Complexes: an Adiabatic Dynamical Simulation Study. *J. Phys. Chem.* **1992**, *96*, 3188−3191.
(36) Laria, D.; Ciccotti, G.; Ferrario, M. Molecular-Dynamics Study of Adiabatic Proton-Transfer Reactions in Solution. *J. Chem. Phys.* **1992**, *97*, 378−388.
(37) Borgis, D.; Hynes, J. T. Molecular-Dynamics Simulation for a Model Nonadiabatic Proton Transfer Reaction in Solution. *J. Chem. Phys.* **1991**, *94*, 3619−3628.
(38) Borgis, D.; Hynes, J. T. Dynamical Theory of Proton Tunneling Transfer Rates in Solution: General Formulation. *Chem. Phys.* **1993**, *170*, 315−346.
(39) Tully, J. C. Proton-Transfer in Solution - Molecular-Dynamics with Quantum Transitions. *J. Chem. Phys.* **1994**, *101*, 4657−4667.
(40) Laria, D.; Ciccotti, G.; Ferrario, M.; Kapral, R. Molecular-Dynamics Study of Adiabatic Proton-Transfer Reactions in Solution. *J. Chem. Phys.* **1992**, *97*, 378−388.
(41) Choi, C. H.; Re, S.; Feig, M.; Sugita, Y. *Chem. Phys. Lett.* **2012**, *539−540*, 218−221.
(42) Gordon, M. S.; Slipchenko, L.; Li, H.; Jensen, J. H. The Effective Fragment Potential: a General Method for Predicting Intermolecular Interactions. *Annu. Rep. Comput. Chem.* **2007**, *3*, 177−193.
(43) Gordon, M. S.; et al. Fragmentation Methods: a Route to Accurate Calculations on Large Systems. *Chem. Rev.* **2012**, *112*, 632−672.
(44) Choi, C. H.; Re, S.; Rashid, M. H. O.; Li, H.; Feig, M.; Sugita, Y. Solvent Electronic Polarization Effects on Na^+−Na^+ and Cl^-−Cl^- Pair Associations in Aqueous Solution. *J. Phys. Chem. B* **2013**, *117*, 9273−9279.
(45) Uddin, N.; Choi, T. H.; Choi, C. H. Direct Absolute pKa Predictions and Proton Transfer Mechanisms of Small Molecules in Aqueous Solution by QM/MM-MD. *J. Phys. Chem. B* **2013**, *117*, 6269−6275.
(46) Ghosh, M. K.; Uddin, N.; Choi, C. H. Hydrophobic and Hydrophilic Associations of a Methanol Pair in Aqueous Solution. *J. Phys. Chem. B* **2012**, *116*, 14254−14260.
(47) Ghosh, M. K.; Re, S.; Feig, M.; Sugita, Y.; Choi, C. H. Interionic Hydration Structures of NaCl in Aqueous Solution: a Combined Study of Quantum Mechanical Cluster Calculations and QM/EFP-MD Simulations. *J. Phys. Chem. B* **2013**, *117*, 289−295.
(48) Ma, Z.; Tuckerman, M. E. On the Connection Between Proton Transport, Structural Diffusion, and Reorientation of the Hydrated Hydroxide Ion as a Function of Temperature. *Chem. Phys. Lett.* **2011**, *511*, 177−182.
(49) Hyeong Lee, Du; Choi, C. H.; Choi, T. H.; Sung, B. J.; Kang, H. Asymmetric Transport Mechanisms of Hydronium and Hydroxide Ions in Amorphous Solid Water: Hydroxide Goes Brownian While Hydronium Hops. *J. Phys. Chem. Lett.* **2014**, 2568−2572.
(50) Smith, R. S.; Kay, B. D. Self-Diffusivity of Amorphous Solid Water Near 150 K. *Chem. Phys.* **2000**, *258*, 291−305.
(51) Head-Gordon, M.; Pople, J. A.; Frisch, M. J. MP2 Energy Evaluation by Direct Methods. *Chem. Phys. Lett.* **1988**, *153*, 503−506.
(52) Raghavachari, K.; Trucks, G. W.; Pople, J. A.; Head-Gordon, M. A Fifth-Order Perturbation Comparison of Electron Correlation Theories. *Chem. Phys. Lett.* **1989**, *157*, 479−483.
(53) Schmidt, M. W.; Baldridge, K. K.; Boatz, J. A.; Elbert, S. T.; Gordon, M. S.; Jensen, J. H.; Koseki, S.; Matsunaga, N.; Nguyen, K. A.; Su, S.; et al. General Atomic and Molecular Electronic Structure System. *J. Comput. Chem.* **1993**, *14*, 1347−1363.
(54) Zhao, Y.; Truhlar, D. G. Density Functionals with Broad Applicability in Chemistry. *Acc. Chem. Res.* **2008**, *41*, 157−167.
(55) Choi, C. H.; Kertesz, M.; Karpfen, A. Limitations of Current Density Functional Theories for the Description of Partial Pi-Bond Breaking. *Chem. Phys. Lett.* **1997**, *276*, 266−268.
(56) Choi, C. H.; Kertesz, M.; Karpfen, A. The Effects of Electron Correlation on the Degree of Bond Alternation and Electronic Structure of Oligomers of Polyacetylene. *J. Chem. Phys.* **1997**, *107*, 6712.
(57) Zhao, Y.; González-García, N.; Truhlar, D. G. Benchmark Database of Barrier Heights for Heavy Atom Transfer, Nucleophilic Substitution, Association, and Unimolecular Reactions and Its Use to Test Theoretical Methods. *J. Phys. Chem. A* **2005**, *109*, 2012−2018.
(58) Marx, D.; Tuckerman, M. E.; Parrinello, M. Solvated Excess Protons in Water: Quantum Effects on the Hydration Structure. *J. Phys.: Condens Matter* **2000**, *12*, A153−A159.